Fractal Structure of Equipotential Curves on a Continuum Percolation Model

Shigeki Matsutani,* Yoshiyuki Shimosako, and Yunhong Wang†
Analysis techology center, Canon Inc. 3-3-20, Shimomaruko, Ota-ku, Tokyo 146-8501, Japan
(Dated: July 18, 2011)

We numerically investigate the electric potential distribution over a two-dimensional continuum percolation model between the electrodes. The model consists of overlapped conductive particles on the background with an infinitesimal conductivity. Using the finite difference method, we solve the generalized Laplace equation and show that in the potential distribution, there appear the *quasi-equipotential clusters* which approximately and locally have the same values like steps and stairs. Since the quasi-equipotential clusters has the fractal structure, we compute the fractal dimension of equipotential curves and its dependence on the volume fraction over $[0, 1]$. The fractal dimension in [1.00, 1.257] has a peak at the percolation threshold p_c.

PACS numbers: 05.10.-a, 05.10.Ln, 05.60.Cd, 64.60.ah, 72.80.Ng, 73.22.-f

I. INTRODUCTION

In the series of articles [1, 2], we have studied the electric conductivity of a percolation model using the finite difference method (FDM) [3]. The purpose of these studies is to reveal the electric properties over the continuum percolation model (CPM). As we explored three dimensional shape effects on the conductivity on CPMs in the previous articles [1, 2], in this article we investigate the fractal properties of the the solutions of the two dimensional generalized Laplace equation,

$$\nabla \cdot \sigma \nabla \phi = 0, \tag{1}$$

for the conductivity distribution $\sigma(x, y)$ of CPM. Recently materials consisting of the conductive particles in a base material with extremely high resistance are studied [4–6]. We handle the binary local conductivities $\sigma(x, y)$ of the binary materials in CPM, i.e., conductive particles on the background with an infinitesimal conductivity. The infinitesimal conductivity i.e., the extremely high resistance, avoids indeterminacy of the solutions of (1) all over there, because approaching to zero differs from the zero itself.

Two dimensional CPMs of the overlapped circles were studied well in Refs.7 and 8 and references therein. In this article, we also deal only with CPM whose particles are overlapped circles with the same radius.

Since the solution of the generalized Laplace equation (1) provides the electric potential distribution, we show that there exist *quasi equipotential clusters*, in which the potential behaves like steps and stairs approximately. There are many pieces whose potentials are approximately flat because the electric connections are very small and thus the resistance is so high at the boundary whereas the inner resistance of the particle or the composite particles are much small.

The existences of the quasi-equipotential clusters means the anomalous behaviors of the equipotential curves. Though the relation between the percolation cluster and fractal structure has been studied [8], in this article, we provide the results how the fractal dimension of the equipotential curves behaves depending on the volume fraction $p \in [0, 1]$. Under the percolation threshold p_c, our computation can read the computation of dielectric behavior on a random configuration of metal particles in the dielectric matter, which was reported in Refs. 9 and 10 if we interpret the conductivity as the dielectric constant.

Contents in this article are as follows. Sec. II shows our computational method; Sec. II.A is on the geometrical setting in CPMs and Sec. II.B gives the computational method of the conductivity over CPMs using FDM, which is basically the same as that in the previous article [1]. Sec. III shows our computational results of the solutions of (1) in CPMs and discuss our results from physical viewpoints.

II. COMPUTATIONAL METHOD

In this section, we explain our computational method of CPM. Though we deal only with two dimensional case, its essential is the same as the three dimensional case using FDM [3] whose detail is in the previous article [1].

A. Geometrical setting

We set particles parameterized by their positions (x, y) into a box-region $\mathcal{B} := [0, x_0] \times [0, y_0]$ at random and get a configuration $\mathfrak{R}_n$ as one of CPMs. In this article, we set $x_0 = y_0 = L = 100$. The particle corresponds to a stuffed circle with the same radius $\rho = 1$, $B_{x_i,y_i} := \{(x, y) \in \mathcal{B} \mid |(x, y) - (x_i, y_i)| \le \rho\}$. The configuration $\mathfrak{R}_n$ is given by $\mathfrak{R}_n := \bigcup_{i=1}^{n} B_{x_i,y_i}$, where each center (x_i, y_i) is given at uniform random in $\mathcal{B}$. We allow their overlapping.

*Electronic address: matsutani.shigeki@canon.co.jp
†Present address Microcreate System Co., 2-1-15 4C, Chuou Yamato Kanagawa 242-0021 Japan.

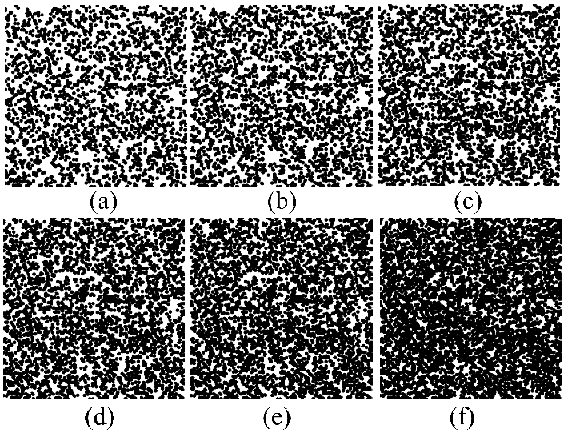

FIG. 1: The configurations of the seed $i_s = 1$ with the volume fractions 0.5, 0.55, 0.6, 0.65, 0.7, 0.8 for (a), (b), (c), (d), (e), (f) respectively.

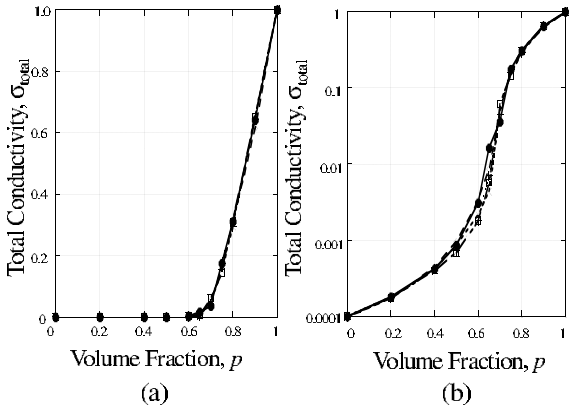

FIG. 2: Conductivity curves; (a) for the linear total conductivity $\sigma_{\rm total}$ and (b) for its logarithm scale.

By monitoring the total volume fraction which is a function of $\mathfrak{R}_n$ and is denoted by $\mathrm{Vol}(\mathfrak{R}_n)$, we continue to put the particles as long as $\mathrm{Vol}(\mathfrak{R}_n) \leq p$ for the given volume fraction p. We find the step $n(p)$ such that $\mathrm{Vol}(\mathfrak{R}_{n(p)-1}) \leq p$ and $\mathrm{Vol}(\mathfrak{R}_{n(p)}) > p$. Since the difference between $\mathrm{Vol}(\mathfrak{R}_{n(p)-1})$ and $\mathrm{Vol}(\mathfrak{R}_{n(p)})$ is at most 3×10^{-4} for the employed parameters. Thus we regard $\mathrm{Vol}(\mathfrak{R}_{n(p)})$ as each p hereafter under this accuracy.

Since we use the pseudo-randomness to simulate the random configuration $\mathfrak{R}_{n(p)}$ for given p, the configuration $\mathfrak{R}_{n(p)}$ depends upon the seed i_s of the pseudo-random which we choose and thus let it be denoted by $\mathfrak{R}_{p,i_s}$. For the same seed i_s of the pseudo-random a configuration $\mathfrak{R}_{p,i_s}$ of a volume fraction p naturally contains a configuration $\mathfrak{R}_{p',i_s}$ of $p' < p$ due to our algorithm. Hence the elements in the set of the configurations $\{\mathfrak{R}_{p,i_s} \mid p \in [0,1]\}$ with the same seed i_s are relevant. Fig. 1 illustrates the configurations of the seed $i_s = 1$ for several p.

B. Computation of the potentials in CPM

To apply FDM to the generalized Laplace equation in CPM, we use a 2000×2000 lattice to represent the square-region $\mathcal{B}$. The radius of the particle $\rho = 1$ corresponds to 25 meshes.

Further we set the binary local conductivities $\sigma(x, y)$ which consists of the conductive particles with the conductivity density $\sigma_{\rm mat} = 1$, and the background with infinitesimal conductivity $\sigma_{\rm inf} = 10^{-4}$.

In order to compute the potential distribution $\phi(x, y)$, we set $\phi = 1$ and $\phi = 0$ on the upper and the lower segments respectively as the boundary condition corresponding to the electrodes. As the side boundary condition, we use the natural boundary for each y-boundary so that at the side boundaries, current normal to each boundary vanish.

Following our algorithm of FDM as mentioned in detail in Ref.1, we numerically solve the generalized Laplace equations (1) for the conductivity distribution $\sigma(x, y)$ for each $\mathfrak{R}_{p,i_s}$.

Then we obtain the total conductivity $\sigma_{\rm total}$ of the system after we integrate the current $\sigma\nabla\phi$ over the line parallel to the x-axis. Since $\sigma_{\rm total}$ is determined for each $\mathfrak{R}_{p,i_s}$, $\sigma_{\rm total}$ is a function of the volume fraction p and the seed i_s of the pseudo-random. We denote it by $\sigma_{\rm total}(p)$.

The dependence of the total conductivities on the volume fraction as a conductivity curve is given by

$$\sigma_{\rm total}(p) = \begin{cases} \frac{(p-p_c)^t}{(1.0-p_c)^t}, & \text{for } p \in [p_c, 1], \\ 0 & \text{otherwise,} \end{cases} \tag{2}$$

where the p_c is the threshold and t is the critical exponent, or merely exponent. Since the threshold p_c and the exponent t are determined by $\{\mathfrak{R}_{p,i_s} \mid p \in [0,1]\}$, they are also functions of the volume fraction p and the seed i_s of the pseudo-random.

III. THE RESULTS AND DISCUSSIONS

A. Conductivity curve

The ordinary computations of the conductivity over the percolation system are performed using the Y-Δ algorithm[11] by assuming that the the conductivity of the background insulator vanishes [12], in other words, (1) is not defined over there in the ordinary approaches.

In our computations using FDM, we handle the binary conductivities $\sigma(x, y)$ due to the demands of the recent material science [4–6].

Even though we deal with the binary conductivities with finitely different resistances, the conductivity curve is naturally obtained as in Fig. 2 and obeys the (1) which exhibits the properties of the percolation system, because the ratio between the binary conductivities $\sigma_{\rm mat}$ and $\sigma_{\rm inf}$ is sufficiently large. Fig. 2 (a) exhibits the linear scale behavior of the total conductivity whereas Fig. 2 (b) shows

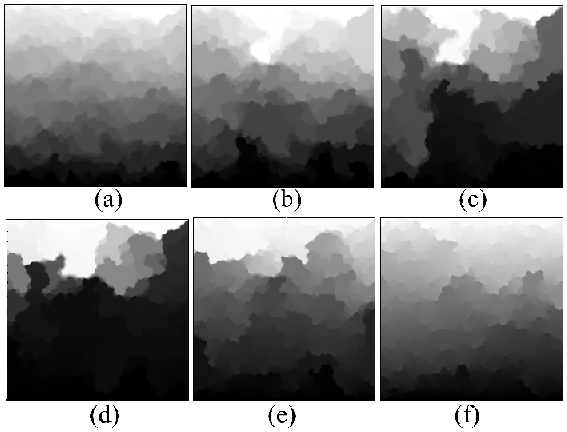

FIG. 3: Potential distributions of the seed $i_s = 1$ with the volume fractions 0.5, 0.55, 0.6, 0.65, 0.7, 0.8 for (a), (b), (c), (d), (e), (f) respectively. The black corresponds to $\phi = 0$ whereas the white does to $\phi = 1$. The graduated gray interpolates them. The quasi-potential clusters exist there.

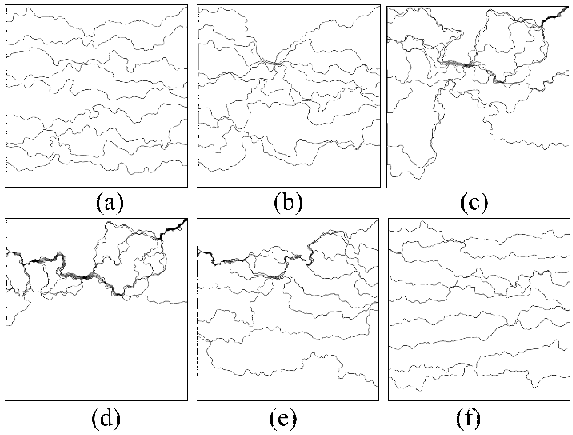

FIG. 4: Equipotential curves of the potential distributions of the seed $i_s = 1$ with the volume fractions 0.5, 0.55, 0.6, 0.65, 0.7, 0.8 for (a), (b), (c), (d), (e), (f) respectively. The curves correspond to the values $\phi = 0.1, 0.2, \ldots, 0.8$, and 0.9.

the logarithm properties. Even though the Fig. 2 (b) illustrate the properties of the binary materials, the linear scale behavior of the total conductivity is described well by (2). We computed twenty cases with different seeds i_s of the pseudo-randomness and determine the threshold p_c and the exponent t using the least mean square method for the points $p > 0.6$. For the simpicity, in this article, we display only the first five cases as in Fig. 2 because they represent the others well.

The average of the percolation threshold is 0.66 ± 0.01 which slightly differs from 0.674 ± 0.04, 0.688 ± 0.005, 0.676 ± 0.002, 0677 and 0.691 which are reported in Ref 7 and the exponent is given as 1.33, which recovers the universal value 4/3 of two-dimensional percolation [7] with this accuracy. Since the effect of the finite size of the analyzed region makes the threshold smaller, the difference comes from the finite size effect [1, 2] but is not essential.

B. Potential distribution

By numerically solving (1), we obtain the potential distribution $\phi(x, y)$ for each volume fraction $p \in [0, 1]$ and the seed of the pseudo-randomness as we display the results in Fig. 3. Fig. 4 shows its equipotential curves for $\phi = 0.1, 0.2, \ldots, 0.9$.

Fig. 5 is parts of Fig. 4 with the configurations of particles at $p = 0.5 < p_c$ and $p = 0.8 > p_c$. The contours basically run to avoid the conductive particles due to the difference of the conductivity. Especially in Fig. 5 (a) for the case $p = 0.5$, the avoidance explicitly appears.

On the other hand, at $p = 1$, the potential is simply described by $\phi(x, y) = y/y_0$ and the contours penetrate into the conductive particles. Thus even for $p = 0.8$, the contours penetrate into the conductive particles on the conductive paths i.e., the percolation clusters which

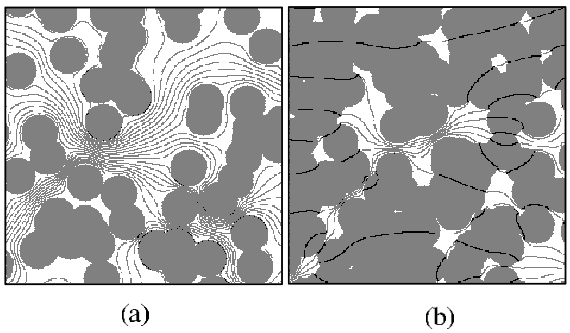

FIG. 5: The equipotential curves with $\delta\phi = 6.01$, and the configurations of particles; (a) for $p = 0.5$ and (b) for $p = 0.8$.

are connected with both anode and cathode. However around the isolated percolation cluster which is not connected with electrodes, the contours go through the gaps among the conductive particles. Fig. 5 (b) contains the similar states to those situations, in which the contours partially penetrate into the conductive particles and partially avoid the conductive particles. However due to the above considerations, these behaviors in Fig. 5 (b) can be naturally interpreted.

Further Fig. 5 shows that the local equipotential curves depends upon the local configurations of these particles. For given resolution and local region, the sets of particles surrounding the region locally play the role of the electrodes but the direction of the locally averaged gradient, i.e., the local electric field, strongly depends upon the resolutions and upon the region which we average. Since XY-model which is the O(2) valued spin system also have the fractal structure [13], the randomness brings the self-similar structure into our system.

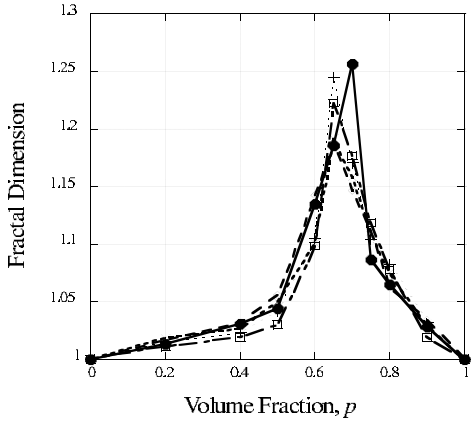

FIG. 6: The fractal dimension v.s. volume fraction p for five seeds.

As Mandelbrot showed that the fractal picture is related to geographical geometry in Ref. 14, Fig. 3 looks like pictures of the piled up mountains in distance using the monochrome water-painting. There are many pieces whose potentials are approximately flat, like leaves of the piled leaves. These properties are interpreted that there exist quasi-equipotential clusters whose individual potential is approximately same and behaves like steps and stairs. In other words, the electric connections among the pieces are very small and thus the resistance is so high at the connections whereas the inner resistance of the particle or the composite particles is much small.

C. Fractal dimension of equipotential curves

Let us consider the effect of the quasi-equipotential clusters on the equipotential curves in Figs. 4 and 5.

Under the threshold p_c, this phenomenon is essentially the same as the one of dielectric properties related to the electric breakdown, which were studied by Gryure and Beale in Ref. 9 and recently by Stoyanov, Mc Carthy, Kollosche and Kofod in Ref. 10, though the authors handled the hard core model in which the overlapping is prohibited instead of our soft core CPMs. They studied the dielectric materials as background with infinite dielectric particles (metal particles), which are governed by the same generalized Laplace equation (1), though it is for the region of $p \in [0, p_c]$. Fig. 5 (a) corresponds to the Fig. 1. in Ref. 9 if the conductivity reads the dielectric constant.

In our computational condition on the conductivity, we can determine the potential distributions over $\mathcal{B}$ for every volume fraction $p \in [0, 1]$ due to the infinitesimal conductivity $\sigma_{\rm inf}$.

As objects in the percolation theory exhibit the fractal structures, related to the percolation clusters [8], related to the breakdown [15–18] and so on, the fractal dimension characterizes these properties. We also computed the fractal dimensions but especially ones of the *equipotential curves*. We used the box-counting method [14]. Since the curves in Fig. 4 of the seed $i_s = 1$ have the fractal structure, their fractal dimensions are not trivial.

The dependences of the fractal dimensions of the equipotential curves on the volume fraction $p \in [0, 1]$ for five different seeds i_s are presented in Fig. 6. Mandelbrot showed that the geographical curves like the coastlines sometimes behave fractal [14] and have the fractal dimensions 1.0∼1.25. Our fractal dimension is in [1.00, 1.257] and has a peak at the threshold p_c. In other words, around p_c, the equipotential curves behave complicatedly and have the self-similar structures. On the other hand, for the $p = 0$ and $p = 1$ cases, the dimension must be equal to 1. Thus the shape of the graph in Fig. 6 shows the curve with a peak at the percolation threshold $p = p_c$.

[1] S. Matsutani, Y. Shimosako, and Y. Wang, Int. J. Mod. Phys. C **21**, 709 (2010).
[2] S. Matsutani, Y. Shimosako, and Y. Wang, arXiv.1107.2158.
[3] R. J. LeVeque, *Finite Difference Methods for Ordinary and Partial Differential Equations* (SIAM, Philadelphia, 1955).
[4] M. H. Al-Saleh and U. Sundararaj, Eur. Polymer J. **44**, 1931 (2008).
[5] D. Tee, M. Mariatti, A. Azizan, C. See, and K. Chong, Comp. Sci. Tech. **67**, 2584 (2007).
[6] Y. Konishi and M. Cakmak, Polymer **47**, 5371 (2006).
[7] M. B. Isichenko, Rev. Mod. Phys. pp. 961–1043 (1992).
[8] D. Stauffer and A. Aharony, *Introduction to percolation theory, revised second ed.* (CRC, Boca Raton, 1991).
[9] M. F. Gyure and P. D. Beale, Phys. Rev. B. **40**, 9533 (1989).
[10] H. Stoyanov, D. M. Carthy, M. Kollosche, and G. Kofod, Appl. Phys. Lett. **94**, 232905 (2009).
[11] D. E. Johnson, J. R. Johnson, J. L. Hilburn, and P. D. Scott, *Electric Circuit Analysis, third ed.* (John Wiley & Sons, New York, 1997).
[12] E. J. Garboczi, M. F. Thorpe, M. S. DeVries, and A. R. Day, Phys. Rev. A **43**, 6473 (1991).
[13] H. Kroger, Phys. Rep. **323**, 81 (2000).
[14] B. Mandelbrot, *Fractal Geometry of Nature* (Times Books, New York, 1982).
[15] F. Peruani, G. Solovey, I. M. Irurzun, E. E. Mola, A. Marzocca, and J. L. Vicente, Phys. Rev. E **67**, 066121 (2003).
[16] A. Palevski and G. Deutscher, J. Phys. A **17**, L895 (1984).
[17] J. Fournier, G. Boiteux, and G. Seytre, Phys. Rev. B **56**, 5207 (1997).
[18] R. Lenormand, Proc. Royal Soc. of London Ser. A **423**, 159 (1989).